UNIVERSITY OF ALBERTA

Department Of Electrical and Computer Engineering

Capstone Project MINT 709

Detection Performance of Wireless Sensor Networks with Multiple Antennas in Fading Channels

Master of Science

In

Internetworking

Submitted By

Kavin Natesan

natesan@ualberta.ca

Supervisor

Vesh Raj Sharma Banjade

Submitted to

Dr. Mike Macgregor

February 17, 2014

Acknowledgements

The success and final outcome of this project required a lot of guidance and assistance from many people I express my deepest appreciation to all who provided the possibility to complete this project. I am especially grateful to Dr Mike McGregor, Director of the Master of Science in Internetworking program, who has great passion for his students' career development. Thank you for the continuous help, encouragement, and constant supervision and for providing all the facilities to complete the project. I also owe great thanks to my project supervisor Mr. Vesh Sharma Banjade for his constant guidance. He took the time to go through the project at various stages, evaluating and correcting my results and data.

I thank Dr. Chintha Tellambura, Dr. Fair Ivan, and Mr. Paul Lu, for providing me with knowledge in the field of networking, and Mr. Shahnawaz Meer for mentoring and providing a real-time technical experience in the laboratory. Thanks to Ms. Sharon Gannon, the program advisor who was in constant touch during the course, and who helped me a lot in planning my courses every semester.

A special thanks to the University of Alberta AICT department for providing me with information technology and all the facilities and software required to finish this project. Finally, I thank my parents whose support and encouragement over the years was the greatest motivation.

Abstract

The problem of distributed detection and decision fusion in wireless sensor networks (WSNs) is revisited. The detection performance of a WSN is inherently limited by the wireless propagation environment. The fusion of decisions forwarded by each sensor is subject to Nakagami-*m* fading which can represent a wide variety of wireless propagation environments. As wireless fading adversely affects the detection performance of any WSN, effective measures to mitigate its impact are needed. Motivated by the benefits of multiple antennas in wireless communications networks in reducing the impact of fading, the integration of multiple antennas at the sensor nodes is considered in this project to improve the detection performance of the WSN. An analytical expression for the optimal log-likelihood ratio (LLR) based fusion rule with multiple antenna based sensor nodes is derived. Numerical results show encouraging performance gains of such WSNs in fading environments compared to the traditional single antenna based WSNs described in the literature. Although LLR based decision fusion is optimal, its demand for channel state information (CSI) is high. To reduce such demand without sacrificing too much detection performance, two suboptimal decision fusion rules, the maximal ratio combining (MRC) and equal gain combing (EGC), that do not require any CSI, are considered in the context of sensor nodes equipped with multiple antennas. Simulation results show that, as expected, the LLR has the best performance among all three rules. The EGC rule outperforms the MRC rule in regions with moderate to high signal-to-noise ratio (SNR) whereas at low SNR the MRC is better than the EGC. The use of multiple antennas was found to be beneficial regardless of the fusion rule employed and yielded significant performance improvement, helping to mitigate the impact of fading on the quality of decision making in a WSN.

Table of contents

List of figures

List of tables

List of acronyms

WSN- Wireless sensor networks

FC - Fusion center

BS - Base station

MRC- Maximal ratio combining

EGC -Equal gain combining

LLR - Log-likelihood ratio

POI - Phenomenon of interest

MCS - Monte Carlo simulation

MIMO - Multiple input and multiple output

DF - Decision fusion

AUC - Area under curve

SNR – Signal-to noise-ratio

ROC - Receiver operating characteristics

LOS - Line of sight

CSI - Channel state information

PDF – Probability density function

List of symbols

N	Number of sensors
L	Number of antennas
P_d	Probability of detection
P_f	Probability of false alarm
P_{md}	Probability of misdetection
P_{dk}	Probability of detection for *k-th* sensor
P_e	Probability of error
n_k	Additive white Gaussian noise
h	Rayleigh fading channel
y	Received signal
γ	Signal-to-noise ratio (SNR)
$\bar{\gamma}$	Average SNR
h_k	Fading channel amplitude
σ^2	Variance
H_1	Signal present
H_0	Signal absent
m_k	Fading parameter for *k-th* sensor
m	Fading parameter
u_k	Local sensor decision

Chapter 1

Introduction

1.1 Motivation

Sensor are small, inexpensive, low-power distributed devices that transduce physical phenomena into signals that can be observed and recorded by a user, are key elements in modern technological advancement. Some examples are: (i) motion sensors—based on infrared, ultrasonic, and microwave technologies—can be used in videogames and for security detection; (ii) electrochemical biosensors are used to test the safety of food and water; and (iii) light sensors detect the presence, absence, or intensity of a light source. An interconnection of sensors, or a sensor network, consists of a small number of low power sensor nodes that are all connected to a central processing unit which consists of on-board sensors, processor, memory, transceivers, and a power supply. However, in today's mobile culture, the flexibility of wireless sensor nodes offers more advantages than wired nodes.

A wireless sensor network (WSN) consists of a large number of wireless sensors spatially distributed across the area that is to be monitored. Each sensor has the capability of communication and has the intelligence necessary for signal processing and networking of data. Recent developments in semiconductors, networks, and power management have driven a large scale deployment of wireless sensors, making them popular in the modern day information communication paradigm [1]. Typical wireless sensor network applications include [2]:

(i) Military Applications

- Battlefield surveillance, e.g., reconnaissance of opposing forces and terrain

(ii) Automotive Applications

- Measurement in chambers and rotating parts, conditions monitoring, e.g., at a bearing

(iii) Building Monitoring

- Monitoring climate changes
- Thermostats and temperature sensing
- Sensing of vibration that could damage the structure of a building

(iv) Environmental Applications

Sensor networks can be used to monitor environmental changes, for example, water pollution detection in a lake that is located near a factory that uses chemicals. Sensor nodes could be randomly deployed in unknown and hostile areas to relay the exact origin of a pollutant. Other examples include forest fire detection, air pollution, and rainfall observation in agriculture.

A sensor has the capability to detect signals and network the data collected. The data collection process involves gathering a stream of data from the sensor nodes and storing the data at a remote location for monitoring purposes. Sensors gather the information or sense the phenomenon of interest (for example, a radar system can detect aircraft or the speed of an automobile) and communicate their data via a wireless medium to the fusion center (FC). The FC processes and combines the information from the sensors and makes a final decision on the presence or absence of the phenomenon of interest.

However, wireless sensors are challenged if signals transmitted from the sensors to the FC over the wireless channel are degraded. Signal degradation can occur because of multipath fading, an inherent phenomenon in wireless propagation that arises due to diffraction, scattering, and reflection of the transmitted wave [3]. Multipath fading can degrade the quality of wireless links and the detection performance of a WSN [1], [2], [4]. Increasing power or employing powerful error correction codes is impractical as WSNs are resource constrained in both energy and bandwidth. However, not much attention has been given to overcoming these defects and improving the detection performance in WSNs. The use of multiple antennas at the sensor nodes might mitigate the impact of fading. This can be achieved by distributed detection, that is, by parallel decision fusion schemes. The fusion of local decisions can be corrupted during the transmission process due to channel fading and this is the focus of this research study. The objectives of this research are described in section 1.2.

1.2 Objectives

The goal of this project is to implement a multiple-antenna technique in a WSN to mitigate the effect of multipath fading and thereby improve its signal detection performance. The main objectives of this project are:

1. To quantify the improvement possible in signal detection performance of a wireless sensor network in generic fading environments by exploiting multiple antenna based sensors.
2. To compare the performance of optimal and suboptimal decision fusion rules deployed at the fusion center in the context of multiple antenna based sensor nodes.

Objectives 1 and 2 are briefly expressed as problems P1 and P2, respectively, in section 1.3.

1.3 Problem statements

P1: The signals received at the FC from each sensor via wireless channels may undergo severe multipath fading and thus the detection performance at the FC will be detrimentally affected. For a WSN with limited resources, the effect of channel fading renders the information unreliable. To this end, multiple antennas, which are known to enhance wireless system performance [12], may be deployed at the sensors to mitigate the impact of fading, and thereby increase the detection reliability. Moreover, the quantification of the improvement possible in detection capability of the sensor network with multiple

antennas is worth investigating.

P2: The FC may combine the received local decisions from the sensors according to two popular paradigms [1]. (i) Optimal decision fusion rule and (ii) Suboptimal decision fusion rule.

The optimal fusion rule comprises log-likelihood ratio (LLR) based fusion which requires the maximum amount of information about the channel in the form of either the channel state or the channel statistics (CS). Although LLR based fusion has the best detection performance it may be too costly to acquire the knowledge of the channel in resource constrained applications [1] such as a WSN which has limited energy (e.g., battery life). This motivates the adoption of suboptimal fusion rules. The suboptimal fusion rules do not require CS as does the optimal LLR, however, there is a slight compromise in performance. In an effort to reduce the complexity of optimal LLR based fusion, two suboptimal fusion rules, maximal ratio combining (MRC) and equal gain combining (EGC), will be investigated for multiple antenna based WSNs.

Chapter 2

Literature Review

2.1 Sensors

A sensor is a device that can convert physical phenomena such as heat, light, motion, vibration, and sound into electrical signals. A sensor may be equipped with relevant transducers so that it can generate an electrical signal depending upon a change in physical, biological, or chemical parameters of interest. Sensors can thus provide a sense of awareness of the surroundings that may be applicable to infrastructure security, habitat monitoring, surveillance, traffic control, etc., specifically in areas where the human based monitoring is not practicable. Thus, the kind of commercial or industrial sensor applied depends on the stimulus and need. Depending upon the corresponding stimulus and the entity of interest, sensors may be used in monitoring temperature, motion, light, electrical changes, chemical, and biological changes (Table I).

Table I. Sensor based on stimulus and the physical entity of interest

Stimulus	Entity
Biological & chemical	fluid concentrations (gas or liquid)
Electric & mechanical	charge, voltage, force, acceleration, torque
Optical	refractive index, reflection, absorption.

2.1.1 Sensor nodes

A smart sensor node combines sensing, processing, and communication components. The traditional architecture of a sensor node is shown in Fig. 1 [24]. The sensing unit (which includes a transducer) detects the change in the parameter of interest and generates an electrical signal which is fed to the signal conditioning circuitry before being fed to the analog-to-digital converter (ADC). The ADC output is input to application algorithms or the processing unit which is also connected to a transceiver that serves as an interface for communicating with other sensors or the central processing unit. The processing unit is responsible for generating a suitable output to the user through the user interface

Thus, an important goal in the development of smart sensor systems is the implementation of systems in a nonintrusive manner so that the information is provided to the user whenever and wherever it is needed.

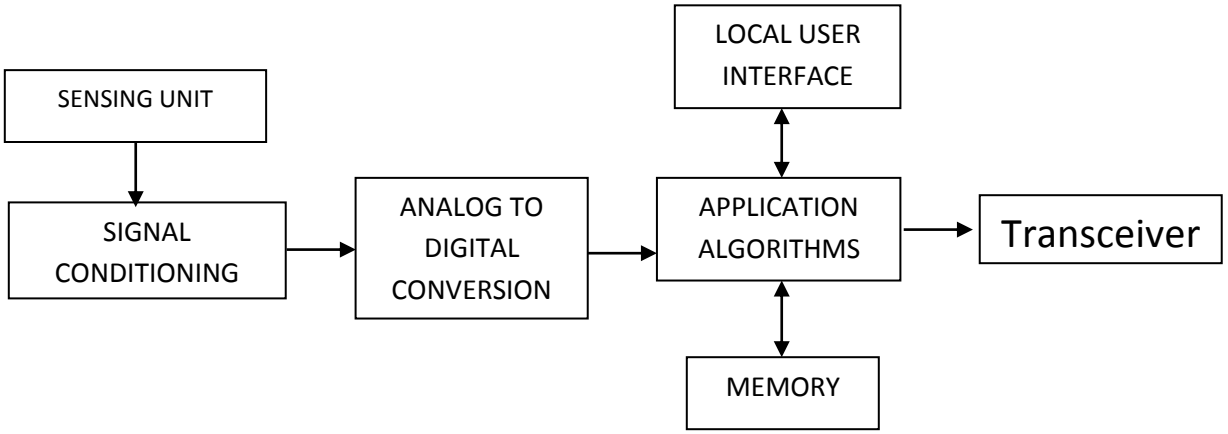

Fig. 1**.** Basic architectural components of a smart sensor [24].

2.2 Wireless Sensor Networks

Traditionally, senor nodes were interconnected by wired links. However, with the rapid proliferation of a demand for service, the number of sensor nodes to be deployed grew very large such that ubiquitous interconnections among the nodes of a device with a wired infrastructure became practically impossible. Moreover, with the advancement of wireless technology, the paradigm for a sensor network shifted toward the incorporation of wireless transmission-reception with the sensor nodes, leading to the formation of wireless interconnections among the nodes, i.e., wireless sensor networks (WSNs).

One of the most attractive features of wireless sensor networks is their autonomy. When deployed in the field, the microprocessor automatically initializes communication with every other node in range, creating an ad hoc mesh network for relaying information to and from the gateway node [6]. This negates the need for costly wiring between nodes, and relies instead on the flexible transmission of information from node to node. This allows nodes to be deployed in almost any location. Moreover, with the development of new wireless technologies, networking protocols, and a growing demand for miniaturized, low-powered, low-cost yet simpler and reasonably efficient wireless communication devices, there has been a growing interest in WSNs for a wide variety of applications ranging from security-sensitive applications to social, military, and environmental problems.

A simple example of a WSN is shown in Fig. 2 where a network of sensor nodes respond to events and requests sent by a phenomenon of interest. The sink node is responsible for broadcasting a request to the whole network and nodes that are intended to reply to the message respond to the broadcast from the sink. As sensor nodes continuously broadcast data to the sink, an independent session needs to be created to collect data and present data from the sensor nodes [6].

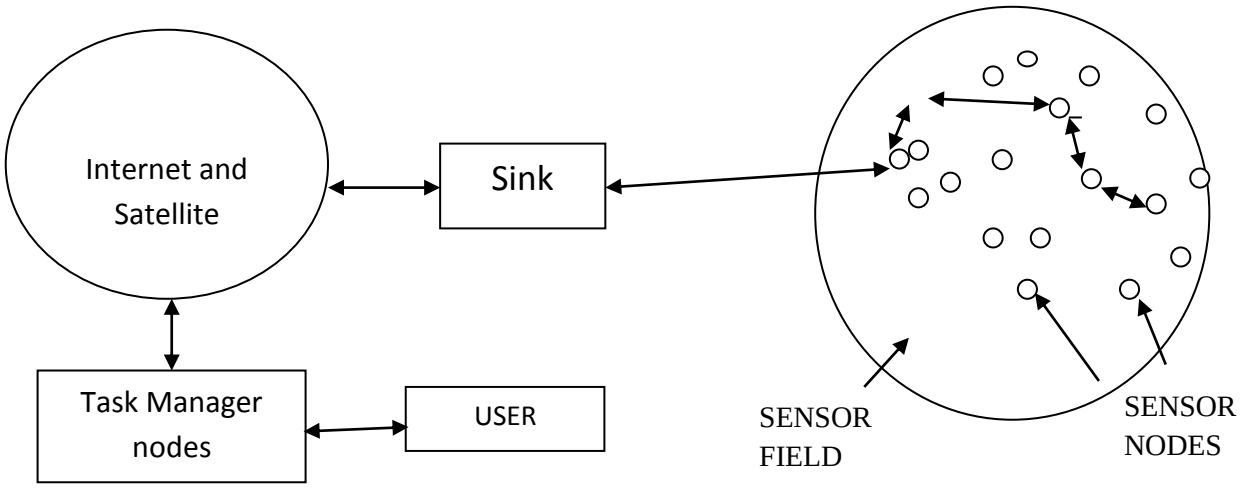

Fig. 2. A WSN communication architecture example.

2.2.1 Issues and Challenges in WSNs

WSNs face technical challenges in deployment, including network discovery, control and routing, information processing, tasking and querying, and security [9]. Other issues faced by WSNs are briefly described below.

- Heterogeneity**:** The devices deployed may be of various types and need to collaborate with each other.
- Distributed processing: The algorithms need to be centralized as the processing is carried out on different nodes.
- Low bandwidth communication: The data should be transferred efficiently between sensors with the goal of consumption of minimum bandwidth.
- Utilization of sensors: The sensors should be utilized in ways that produce the maximum performance and least consumption of energy.
- Real time computation: The computation should be done quickly as new data is always being generated.

The unique features of WSNs, however, trigger further challenges; for example, the lifetime of a sensor node is constrained by the battery attached to it. Moreover, these challenges are

complicated by wireless losses and collisions of data among sensor nodes that are deployed under similar conditions [10]. A major issue faced by WSNs is data loss due to the wireless propagation environment; this loss is primarily due to multipath fading which is a phenomenon inherent in signal propagation in wireless environments and is therefore one of the major focuses in this project. The wireless fading channel and some of the classical models popularly used in depicting wireless channel characteristics are described in section 2.3.

2.3 Wireless fading channel models

Multipath fading is due to the constructive and destructive combination of randomly delayed, reflected, scattered, and diffracted signal components [3]. Fading is one of the major performance degradation factors in wireless systems. For example, in a cellular system, even when the transmitting base station (BS) transmits with a high power, the receiving mobile station may be remote and the signal is affected by surrounding structures in the environment. This degrades the signal quality which is usually measured by the signal-to-noise ratio (SNR). When the SNR is low, the signal does not have high detection probability. A higher SNR value means that the signal strength is stronger in relation to the noise levels, which allows higher data rates and fewer retransmissions – all of which offers better throughput.

Wireless propagation modelling is thus essential in the design of any wireless transmission-reception system. Three classical models that are widely considered to model the wireless fading channel are Rayleigh, Rician, and Nakagami. Fading models are the most commonly used small scale models in wireless communications/WSN [12].

2.3.1 Rayleigh Fading

Rayleigh fading occurs when there is no line of sight between the transmitter and receiver. It is particularly prevalent in scenarios where the signal is scattered between the transmitter and receiver. The Rayleigh fading model can be used to describe the form of fading that occurs when multipath propagation exists. The Rayleigh fading channel is represented by Equation 2.1.

$$p_\gamma(\gamma) = \frac{1}{\bar{\gamma}} \exp\left(-\frac{\gamma}{\bar{\gamma}}\right) \qquad ,\gamma > 0, \tag{2.1}$$

where, γ is the SNR and $\bar{\gamma}$ is the average SNR.

The average enveloper power is $E[\alpha^2] = \Omega_P = 2b_0$, so that

$$p_\alpha(x) = \frac{2x}{\Omega_p} \exp\left(-\frac{x^2}{\Omega_p}\right) \quad ,x \geq 0. \tag{2.2}$$

This type of fading is called Rayleigh fading. The corresponding squared envelope $\alpha^2(t) = |g(t)|^2$ is exponentially distributed at any time t_1 with density

$$p_{\alpha^2}(x) = \frac{1}{\Omega_p} \exp\left(-\frac{x}{\Omega_p}\right). \quad (2.3)$$

The squared-envelope at time *t* is significant because it is proportional to the instantaneously received signal power at time *t* [12].

2.3.2 Rician Fading

In small-scale fading, when the signal arrives at the receiver by several paths and one of them, typically a LoS (line of sight) signal is much stronger than the others, then such channel is termed a Rician fading channel and the amplitude of the received signal is said to be Rice distributed [12]. The Rician distribution is given by

$$p(r) = \left\{\frac{r}{\sigma^2} e^{-\frac{(r^2+A^2)}{2\sigma^2}} I_0\left(\frac{Ar}{\sigma^2}\right)\right\} \ , \ A \geq 0, r \geq 0, \quad (2.4)$$

where parameter A denotes the peak amplitude of the dominant signal and $I_0(\bullet)$ is the modified Bessel function of the first kind at zero-order.

$$p_\alpha(x) = \frac{x}{b_0} \exp\left(-\frac{x^2+s^2}{2b_0}\right) I_0\left(\frac{xs}{b_0}\right) \ , x \geq 0, \quad (2.5)$$

where $s^2 = m_1^2(t) + m_Q^2(t)$ is the nonlinearity parameter [12]. This type of fading is called Rician fading and is often used to describe fading in environments.

The Rice factor, *K*, is defined as the ratio of the LoS or the ratio of specular power s^2 to scattered power $2b_0$, that is, $K = s^2/2b0$. When $K = 0$, there is no LoS or specular component and the envelope exhibits Rayleigh fading. When $K = \infty$, there is no scatter component and the channel does not exhibit any fading. The envelope distribution can be rewritten in terms of the Rice factor and the average envelope power $E[\alpha 2] = \Omega p = s^2 + 2b_0$ by first noting that

$$s^2 = \frac{K\Omega_p}{K+1}, \qquad b_0 = \frac{\Omega_p}{2(K+1)}. \quad (2.6)$$

Substituting s^2 and b_0 in Equation (2.5) yields

$$p_{\alpha^2}(x) = \frac{K+1}{\Omega_p} exp\left\{-K - \frac{(K+1)x}{\Omega_p}\right\} I_0\left(2\sqrt{\frac{K(K+1)x}{\Omega_p}}\right), \ x \geq 0. \quad (2.7)$$

Here, when $K = 0$ it is the Rayleigh probability density function (PDF).

2.3.3 Nakagami-*m* fading

The Nakagami-*m* distribution has gained a lot of attention lately due to its ability to model a wider class of fading channel conditions. The Nakagami distribution was selected to fit empirical data, and is known to provide a close match to experimental data that cannot be fit to either Rayleigh or Rician distributions. More recent studies also showed that Nakagami-*m* gives the best fit for satellite-to-indoor and satellite-to-outdoor wireless communications [13].

The PDF of the Nakagami-m distributed channel is given by

$$P\alpha(x) = \frac{2m^m x^{2m-1}}{\Gamma(m)\Omega_p^m}\exp\left\{-\frac{mx^2}{\Omega_p}\right\}, \qquad m \geq \frac{1}{2}, \tag{2.8}$$

where the squared envelope has a Gamma distribution

$$P\alpha^{\,2}(x) = \left(\frac{m}{\Omega_p}\right)^m \frac{x^{m-1}}{\Gamma(m)}\exp\left\{-\frac{mx}{\Omega_p}\right\}, \tag{2.9}$$

where $\Omega_p = E[\alpha^2]$ and *m* is the Nakagami fading parameter (Fig. 3).

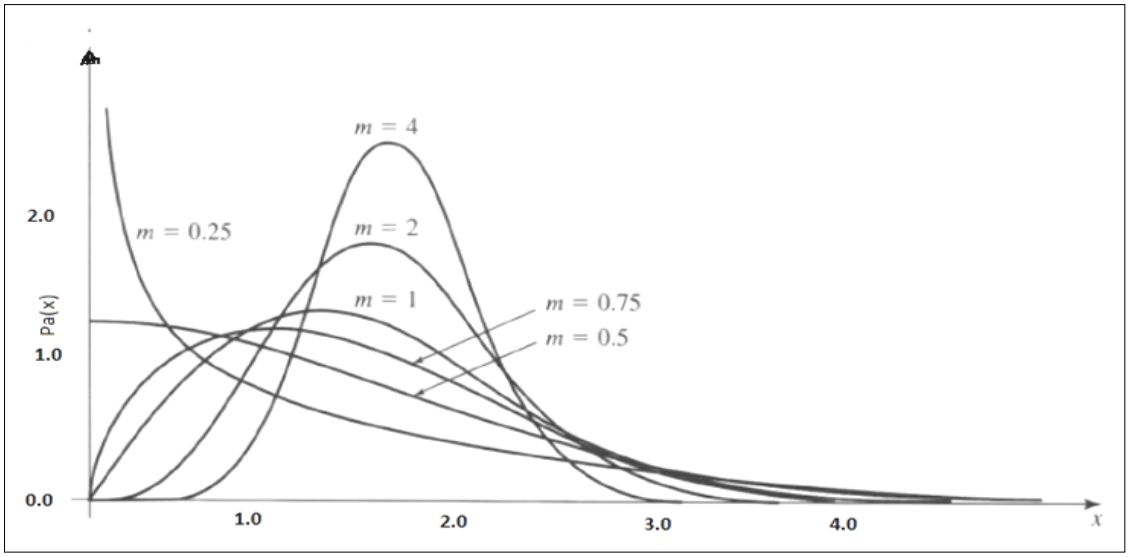

Fig .3. The Nakagami PDF for several values of m with $\Omega_p = 1$ [20].

The Fig. 3 depicts that when there is an increase in the value of m the fading is decreased, thus there is a higher probability of signal detection.

Beyond its empirical justification, the Nakagami distribution is often used for the following reasons. First, the Nakagami distribution can model fading conditions that are either more or less severe than Rayleigh fading. Other special cases are listed below:

When *m* = 1, the Nakagami distribution becomes the Rayleigh distribution; When *m* = 1/2 it becomes a one sided Gaussian distribution; When *m* = ∞ the distribution becomes an impulse (no fading).

Thus, if $m < 1$, the Nakagami-m distributed fading is more severe than Rayleigh fading, and for values of $m > 1$, the fading circumstances are less severe than Rayleigh fading. For the values of m > 1, the Nakagami-*m* distribution closely approximates the Rician distribution, and the parameters m and the Rician factor K (which determines the severity of Rician fading) can be mapped via Equations 2.10 and 2.11 [12].

$$K = \frac{\sqrt{m^2-m}}{m-\sqrt{m^2-m}}, \quad m>1, \tag{2.10}$$

$$m = \frac{(K+1)^2}{(2K+1)}, \quad K \geq 0. \tag{2.11}$$

2.4 Multiple Antennas

Fading converts an exponential dependency of the bit error probability on the average received bit energy-to-noise ratio into an inverse linear dependency, yielding a very large performance loss. Diversity is one very effective remedy that exploits the principle of providing the receiver with multiple independently faded replicas of the same information bearing signal. Some diversity techniques are space, angle, multipath, and time diversity. Space diversity is achieved using multiple transmitter or receiver antennas [12]. The use of multiple antennas at the receiver and the transmitter has become more frequent in wireless communications over the past few years. It has been shown that multiple receiver antennas can improve reception through selection of the stronger signal or by the combination of individual signals at the receiver. The spatial separation between antenna elements at the transmitter and/or receiver is chosen so that the diversity branches experience uncorrelated fading. Multiple antennas can be utilized to accomplish a multiplexing gain or a diversity gain, thus enhancing the bit rate, the error performance, or the signal-to-noise-plus-interference ratio of wireless systems. These multiple-antenna systems, often called multiple-input multiple-output (MIMO) systems (Fig. 4) have multiple antennas from 1 to M at the transmitter side and likewise 1 to N multiple antennas on the receiver side. This system has evolved rapidly because of the improvement in system performance and data rates [22].

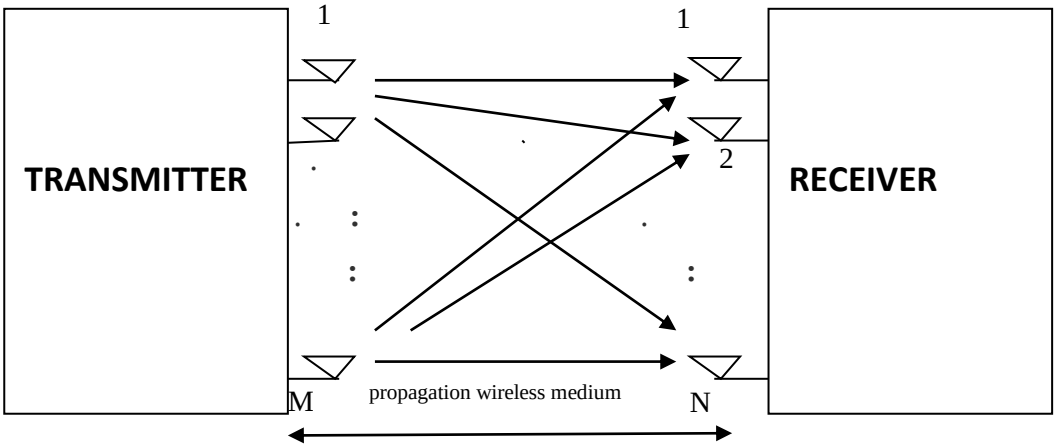

Fig.4. Model of multiple-input multiple-output [12].

Compared to single antenna techniques, it has long been known that multiple antennas can improve reception through selection of the stronger signal or the combination of individual signals at a receiver [14]. Multiple antenna transmission can improve capacity within a given bandwidth by taking advantage of the rich scattering in a typical wireless channel. A channel in a wireless medium can be affected by fading and this will impact the SNR. Because multiple antennas provide the receiver with multiple versions of the same signal, the probability that they will all be affected at the same time is considerably reduced.

2.5 Detection of WSN Performance Metrics

Sensor nodes are organized in a parallel fusion architecture (PFA). Each sensor independently detects the event under observation, generates information, and sends a signal to the FC through a wireless communication link about the presence or absence of a phenomenon of interest (POI).

Two fundamental performance measures of any detector are the probability of detection (P_d) and the probability of false alarm (P_f) these probabilities are calculated at the FC and help to evaluate the performance of the WSN.

Probability of Detection(P_d)

The probability of detection of a signal (object) or a phenomenon of interest by the sensor at a particular point is calculated at the FC.

$$P_d = \mathrm{P}\{\mathrm{H}_1 \text{ decided} / \mathrm{H}_1 \text{ true}\}, \tag{2.12}$$

where $\mathrm{P}\{\mathrm{H}_1 \text{ decided} / \mathrm{H}_1 \text{ true}\}$ is the conditional probability of the position of the target and P_d the probability of detection.

Probability of False Alarm (P_f)

A false alarm is an erroneous sensor target detection decision caused by noise or other interfering signals that exceed the detection threshold. In general, it is an indication of the presence of a sensor target when there is no valid target (POI).

$$P_f = \mathrm{P}\{\mathrm{H}_1 \text{ decided} / \mathrm{H}_0 \text{ true}\} \tag{2.13}$$

where $\mathrm{P}\{\mathrm{H}_1 \text{ decided} / \mathrm{H}_0 \text{ true}\}$ is the conditional probability of the position where a target is not present and P_f is the probability of a false alarm.

2.6 Fusion Schemes

The sensors in a WSN deployed in an environment to sense POI (events) and collect observations, collect and transmit the data over wireless channels to the FC. As shown in (Fig. 5) the FC jointly processes data from local sensors and forms a global decision that is a situational assessment and

sends it to the BS [1]. Decision fusion rules at the FC can be classified as optimal and suboptimal decision fusion schemes.

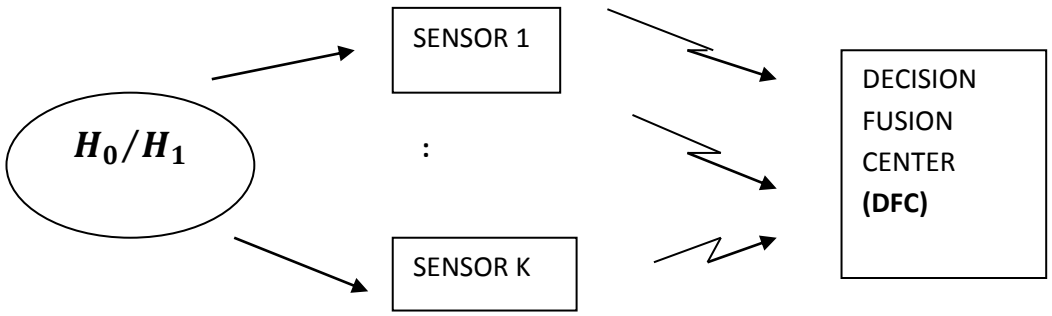

Fig. 5. The decision fusion model of a WSN.

2.6.1 Optimal fusion rules

The fusion rules that help to combine information from various sensors are distributed to sense the events across the environment. The optimal fusion rules are used in a parallel fusion model [4]; the optimal LLR is a rule that is usually implemented. Unfortunately, the optimal decision fusion (DF) rule over MIMO channels with instantaneous CSI presents several difficulties in its implementation: (i) complete knowledge of the channel parameters and sensors local performances is not available; (ii) numerical instability of the formula due to the presence of exponential functions with large dynamics; (iii) exponential growth of complexity with the number of sensors. This motivates a quest for suboptimal DF rules with simpler implementation and reduced system knowledge.

2.6.2 Suboptimal fusion rules

Compared to optimal fusion rules, the suboptimal decision fusion center (DFC) shows less satisfactory performance but requires much less system knowledge. Some of the suboptimal rules are MRC, EGC, Chair-Varshney (C-V). In [4] it is shown for low channel SNR that MRC is optimal. Interestingly, the very simple EGC statistic, which requires a minimum amount of information, outperforms both MRC and Chair-Varshney fusion rules for most values of SNR [1]. The various suboptimal fusion rules and their performance are shown in (Table II)

Table II. Comparison of fusion rules [1]

Fusion static	Prior information required	Performance
LLR	Channel SNR and performance indices	Optimal
MRC	Channel SNR	Near-optimal for low SNR
EGC	NONE	Robust for most SNR range
C-V	Sensor performance indices	Near-optimal for large SNR

Chapter 3

3. Detection Performance of Wireless Sensor Networks with Multiple Antennas in Nakagami-*m* Fading

3.1 Introduction

In this chapter the performance of WSN's with multiple antennas in multipath fading channels is discussed with various simulation and numerical results. The sensors deployed in various environments pass the information sensed (i.e., the POI) to the FC. The signals received at the FC from each sensor via wireless channels may undergo severe multipath fading and thus the detection performance at the FC will be detrimentally affected. For a WSN with limited resources, the effect of channel fading renders the information unreliable.

Multiple antennas that enhance the WSN performance may be deployed at the sensors to mitigate the impact of fading and increase detection reliability. The implementation of multiple antennas at the sensors allows multiple copies of the same signal to be transmitted from each sensor to the FC. Here we also discuss about the optimal decision fusion rules like LLR in WSN's. However with a slight compromise in the performance we adopt the suboptimal decision fusion rules like MRC and EGC which does not require more CSI like the optimal. Comparisons are made between the optimal and suboptimal decision fusion rules to show the effect of their performances.

The rest of chapter is as follows. With the system model described in section 3.2. Expression for Optimum fusion rule at the FC with multiple antennas 3.3. Simulation model with numerical results and discussion in section 3.4. Receiver operating characteristics (ROC) in section 3.5. Comparison of fusion schemes in the quest for high signal detection probability in section 3.6

3.2 System Model

The three layer model for a distributed detection system in the presence of fading channels is illustrated in Fig 10. There are two hypotheses, H_1 and H_0, to be tested: that is, is there a POI (H_1) or is there no POI (H_0). These local decisions are transmitted via fading and noisy channels to a fusion center. For WSNs operating in a fading environment, channel fading and noise impairment may render the received decisions at the fusion center unreliable, especially in resource constrained applications. Toward this end, a channel layer must be incorporated into our model to allow for the development of channel aware decision fusion rules that have proved to be energy efficient [1-4].

Upon receiving its observation, the *k*-th sensor makes a local (hard) decision about the presence (H_1) or absence (H_0) of a phenomenon of interest (POI) based on its observation only. The local sensor decision is denoted by u_k, where u_k = 1 when is H_1 true and $u_k = -1$ when H_0 is true. The reliability of the local sensors is characterized by the probabilities of detection and false alarm, denoted by P_{dk} and P_{fk} , respectively, for the *k*-th sensor [3]. In general, these (P_{dk}, P_{fk}) pairs need not be identical and are functions of the SNR as well as thresholds at local sensors [1-2]. Where h_k is fading channel amplitude**,** n_k is additive white Gaussian noise with variance σ^2. The FC combines the local decisions to make a global decision about the presence or absence of a POI (Fig. 6).

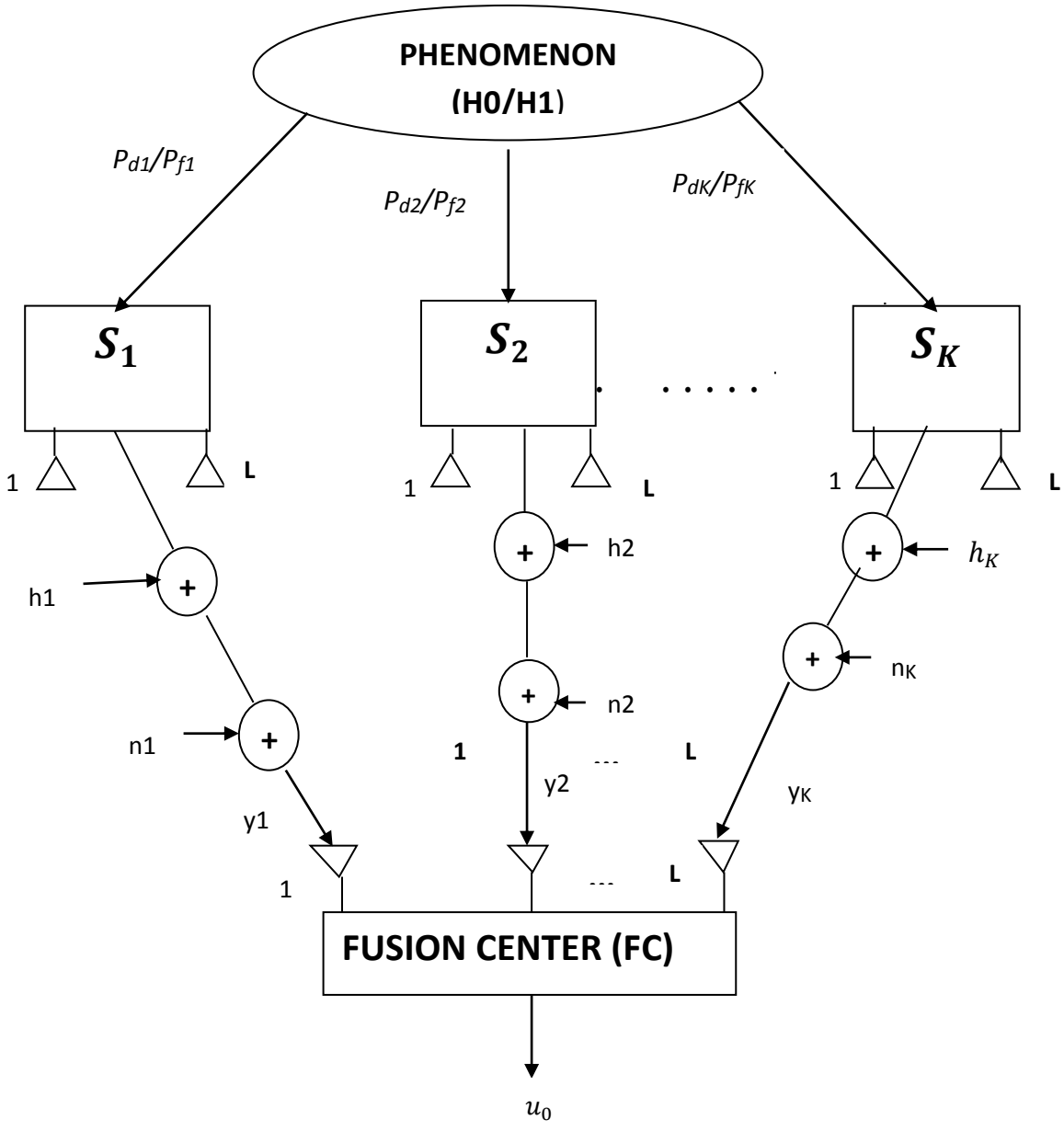

Fig. 6. Parallel fusion model in the presence of fading and noisy channels between local sensors and the fusion center.

In case of H_1 where the signal is present,

$y_{k_l} = x_{k_l} + n_{k_l} = u_{k_l} h_{k_l} + n_{k_l}$ where $k = 1, 2, ..., K$

$y_{k_l} = u_{k_l} h_{k_l} + n_{k_l}$ $l = 1,2,.....L$

here, $u_k = 1|H_1$

$$y_{k_l} = h_{k_l} + n_{k_l}. \quad (3.1)$$

In case of H_0, where the signal is not present,

$y_{k_l} = -x_{k_l} + n_{k_l} = - u_{k_l} h_{k_l} + n_{k_l}$ where $k = 1, 2, ..., K;$

$y_{k_l} = -u_{k_l} h_{k_l} + n_{k_l}$ $l = 1,2,.....L$

here, $u_k = -1|H_0$

$$y_{k_l} = -h_{k_l} + n_{k_l} \quad (3.2)$$

y_k is the received signal vector at the FC from the k-th sensor with L antennas,

$y_k = [y_{k_1}, y_{k_2}, \dots \dots \dots \dots y_{k_L}]$.

where K is the sensor index, L is the antenna index.

In this model we consider a Nakagami-m fading environment, where m is the fading parameter, and the PDF (denoted using the notation $P_X(x)$) of h_k is given by

$$P_{h_k}(h_k) = \frac{2(m_k)^{m_k}}{\gamma(m_k)} h_k^{2m_k-1} exp(-m_k h_k^2), \quad h_k \geq 0 \quad (3.3)$$

We assume throughout that each Nakagami fading channel has unit power, i.e.,

$E[|h_k|^2] = 1$, where E[.] denotes expectation.

3.3 Expression for Optimum fusion rule at the FC with multiple antennas

The proposed LLR (Λ) for multiple antennas is given by the equation

$$\Lambda = \sum_{K=1}^{K} log \left\{ \frac{P(y_{k_1}, y_{k_2}, \dots\dots\dots\dots y_{k_L}|H_1)}{P(y_{k_1}, y_{k_2}, \dots\dots\dots\dots y_{k_L}/H_0)} \right\}. \quad (3.4)$$

Proof:

The joint PDF of the received signals (via L antennas) at the k-th sensor node conditional on the decision made by the node u_k, can be expressed as

$$P(y_{k_1}, \dots y_{k_L}|u_K = 1) = \int_0^\infty \dots \int_0^\infty P(x_{k_1}, \dots x_{k_L}|u_K = 1)\, P(y_{k_1}, \dots y_{k_L}|x_{k_1}, \dots x_{k_L}) dx_{k_1} \dots dx_{k_L}. \quad (3.6)$$

We assume that the received signals at each antenna are statistically independent so that $h_{k_1}, h_{k_2}, \dots h_{k_L}$ and thus $x_{k_1}, \dots x_{k_L}$ are independent. Then, the joint PDF can be expressed as a product of individual PDFs such that

$$P(x_{k_1}, x_{k_2}, \dots x_{k_L}|u_K = 1) = P(x_{k_1}|u_K = 1) \dots\dots P(x_{k_L}|u_K = 1), \quad (3.7)$$

$P(y_{k_1}, \dots y_{k_L}|x_{k_1}, \dots x_{k_L}) = P(y_{k_1}|x_{k_1})\ .\ P(y_{k_2}|x_{k_2}) \dots .\ P(y_{k_L}|x_{k_L})$. (3.8)

Then,

$P(y_{k_1}, y_{k_2}, \dots y_{k_L}|u_K = 1) = \int_0^\infty P(x_{k_1}|u_K = 1).\ P(y_{k_1}|x_{k_1})\, dx_{k_1}$, (3.9)

$$. \int_0^\infty P(x_{k_1}|u_K = 1).\ P(y_{k_1}|x_{k_1})\, dx_{k_1},$$

$$\vdots$$

$$\int_0^\infty P(x_{k_L}|u_K = 1).\ P(y_{k_L}|x_{k_L})\, dx_{k_L}.$$

From [2, eq.(5, 6)] we get

$P(x_{k_L}|u_K = 1) = \frac{2m^m}{\Gamma(m)} x_{K_l}^{2m-1} \exp(-m x_{K_l}^2)$, $x_{K_l} \geq 0$, where $l \in \{1,2, \dots . L\}$. (3.10)

Similarly,

$P(y_{k_l}|x_{k_l}) = \frac{1}{\sqrt{2\pi}.\sigma} e^{-\frac{(y_{k_l} - x_{k_l})^2}{2\sigma^2}}$. (3.11)

By following the steps in [2] and substituting (8) and (7) in (6) we get

$P(y_{k_1} .. y_{k_L}|u_K = 1) = \prod_{l=1}^{L} \sqrt{\frac{2}{\pi}}\ \frac{\gamma(2m) e^{\frac{-y_{K_l}^2}{2\sigma^2}}}{\Gamma(m)\sigma} \left(\frac{m\sigma^2}{2\sigma^2 m+1}\right)^m . \exp\left(\frac{-y_{K_l}^2/4\sigma^2}{2\sigma^2 m+1}\right) D_{-2m}\left(\frac{-y_{K_l}/\sigma}{\sqrt{2\sigma^2 m+1}}\right)$ (3.12)

Similarly,

$P(y_{k_1}, \dots y_{k_L}|u_K = -1) = \prod_{l=1}^{L} \sqrt{\frac{2}{\pi}}\ \frac{\gamma(2m) e^{\frac{-y_{K_l}^2}{2\sigma^2}}}{\gamma(m)\sigma} \left(\frac{m\sigma^2}{2\sigma^2 m+1}\right)^m . \exp\left(\frac{y_{K_l}^2/4\sigma^2}{2\sigma^2 m+1}\right) D_{-2m}\left(\frac{y_{K_l}/\sigma}{\sqrt{2\sigma^2 m+1}}\right)$. (3.13)

From the total probability law,

$P(y_{k_1}, \dots y_{k_L}|H_1) = \sum_{u_k} P(y_{k_1}, \dots y_{k_L}|u_K) P(u_K|H_1)$

$= P(y_{k_1}, \dots y_{k_L}|u_K = 1).P(u_K = 1|H_1) + P(y_{k_1}, \dots y_{k_L}|u_K = -1)\ .P(u_K = -1|H_1)$

$= P(y_{k_1}, \dots y_{k_L}|u_K = 1).P_{d_k} + P(y_{k_1}, \dots y_{k_L}|u_K = -1).(1-P_{d_k})$. (3.14)

$P(y_{k_1}, \dots y_{k_L}|H_0) = \sum_{u_k} P(y_{k_1}, \dots y_{k_L}|u_K) P(u_K|H_0)$

$= P(y_{k_1}, \dots y_{k_L}|u_K = 1).P(u_K = 1|H_0) + P(y_{k_1}, \dots y_{k_L}|u_K = -1)\ .P(u_K = -1|H_0)$

$= P(y_{k_1}, \dots y_{k_L}|u_K = 1).P_{f_k} + P(y_{k_1}, \dots y_{k_L}|u_K = -1).(1-P_{f_k})$. (3.15)

By Substituting (3.14) and (3.15) in (3.4), the LLR becomes

$\Lambda = \sum_{k=1}^{K} log\left[\frac{P(y_{k_1}, \dots y_{k_L}|u_K = 1).P_{d_k} + P(y_{k_1}, \dots y_{k_L}|u_K = -1).(1-P_{d_k})}{P(y_{k_1}, \dots y_{k_L}|u_K = 1).P_{f_k} + P(y_{k_1}, \dots y_{k_L}|u_K = -1).(1-P_{f_k})}\right]$ (3.16)

$$\Lambda = \sum_{k=1}^{K} log\left[\frac{\prod_{l=1}^{L} P_{d\,k}{}^{D-2m}\cdot\left(-A_{K_l}\right)+(1-P_{d\,k})^{D-2m}\cdot\left(A_{K_l}\right)}{\prod_{l=1}^{L} P_{f\,k}{}^{D-2m}\cdot\left(-A_{K_l}\right)+(1-P_{f\,k})^{D-2m}\cdot\left(A_{K_l}\right)}\right], \tag{3.17}$$

where $P_{d\,k}$ and $P_{f\,k}$ are the probability of detection and probability of false alarm of the *k*-th sensor and

$$A_{K_L} = \frac{y_{K\,l}/\sigma}{\sqrt{2\sigma^2 m+1}}. \tag{3.18}$$

The result in (3.17) is the optimum channel statistic combining rule at the FC for a WSN with multiple antennas in a Nakagami-*m* fading environment. Once we have the LLR, the detection and false alarm probabilities can be evaluated by using

$$P_d = \Pr\{\Lambda > \lambda | H_1\},$$

$$P_f = \Pr\{\Lambda > \lambda | H_0\},$$

where λ is the threshold of detection which can be preset depending upon the false alarm probability requirements or can be varied from a low to high value (elaborated more from Section 3.3.1 onwards.)

3.3.1 Detection performance of a WSN in a generic fading environment by exploiting multiple antennas

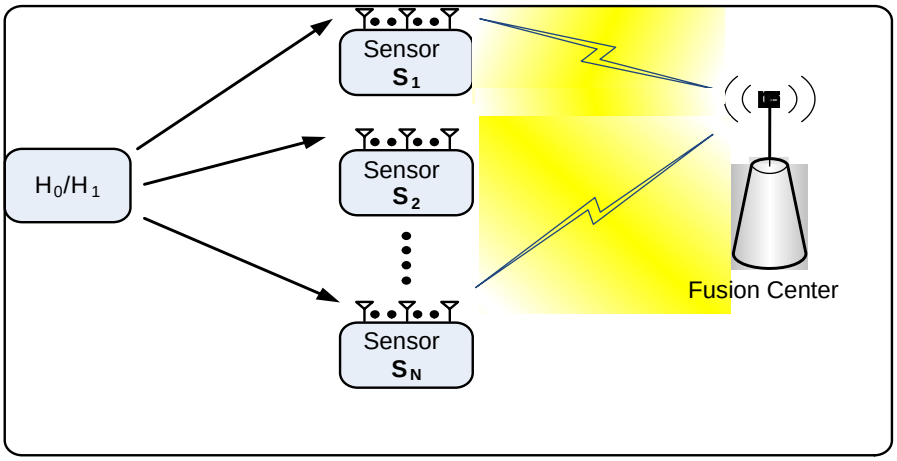

Fig. 7. System model sensors with multiple antennas.

3.4 Simulation model with numerical simulation results and discussion

To obtain results we use a Monte Carlo simulation (MCS). The Monte Carlo method is computational and iterative and relies on repeated random sampling to compute its results. In this project we used the MCS in MATLAB in our experimental work and to verify the results.

In this section, the numerical and simulation results are illustrated to gain meaningful insights for understanding the effect of increase in the number of antennas at the sensor nodes increases the probability of detection (P_d) and increases the performance of the WSN. Several graphical plots are obtained to gain physical insights to show the effect of multiple antennas. The numerical results and the simulation graphs are shown in Fig. 9–18.

3.4.1 Fixing the threshold value in the experiments

With P_{dk} = 0.5 and P_{fk} = 0.05 per sensor. Here we vary the threshold in order to get the value of the probability of false alarm P_f around 0.01, as smaller the P_f, the better the probability of detection P_d. In this case we assigned a threshold value of 6.02 which gives a P_f = 0.01.

We followed the same procedure for P_d vs. SNR with varying L and m values, and for P_d vs. N, $and\ P_{md}$ vs. N, with the same values of P_{dk} and P_{fk} taken into account.

3.4.2 Effect of multiple antennas

The P_d vs. SNR plots in Fig. 8 show the effect of increasing L (number of antennas). In this section, we illustrate both graphically and numerically the performance comparison of single and multiple antennas in WSN's and the percentage increase in the probability of detection with effect of multiple antennas for the simulated plot of P_d vs. SNR. Fig. 8 indicates the possible performance improvement in increasing the number of antennas used in the sensor. Here, the number of antennas on the sensor node L is given values of 1, 2, 3. The probability of detection at the FC is evaluated for a fixed number of sensors (N = 8) as a function of channel SNR. The Nakagami fading parameter m is fixed to a value of 5 throughout the simulation.

From the graph in Fig. 8 which is simulated model for P_d vs. SNR with a number of antennas L = {1,2,3}, we can infer that the WSN performance increases as we keep increasing the antenna count at the sensor node. It also shows that the P_d increases with an increase in the SNR. (i.e., in this graph it is very clear the performance of the WSN is greater with positive values of SNR).

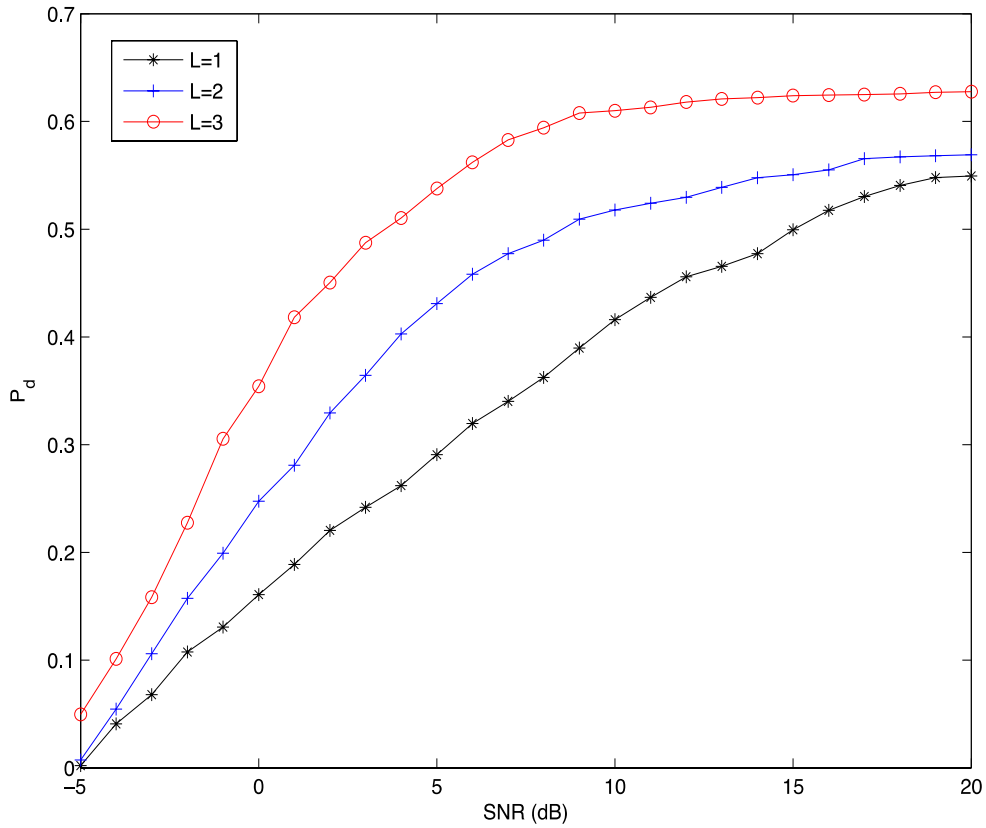

Fig. 8: P_d vs. SNR for varying L with m=5

Performance Quantification

From the graph obtained in Fig. 8, increasing the antenna count from L=1 to L = 2 produces an increase in the average probability of detection (P_d). For example, when SNR = 0 db, P_d with L = 2 has a higher value than P_d with L = 1. The gain in P_d by increasing the antenna count from L = 1 to L = 2 is 53.9%. The gain in P_d by increasing the antenna count from L = 2 to L = 3 is 43.11%. This verifies that the use of multiple antennas at the sensor nodes improves the detection performance under fading environments.

3.4.3 Effect of fading parameter *m*

The P_d vs. SNR plots in Fig. 9 show the effect of m the fading parameter index. In this experiment the probability of detection P_d at optimal LLR for a system with false alarm P_f = 0.01 versus the average SNR per sensor is plotted for different values of m. Here L = 2. Fig.9 depicts that P_d increases with increasing values of m, the Nakagami fading parameter [3] with an increasing range of SNR values. This is because when the fading parameter m is increased from m =1 to m =2 the fading in the channels between the sensors is less, hence there is a better average probability of detection.

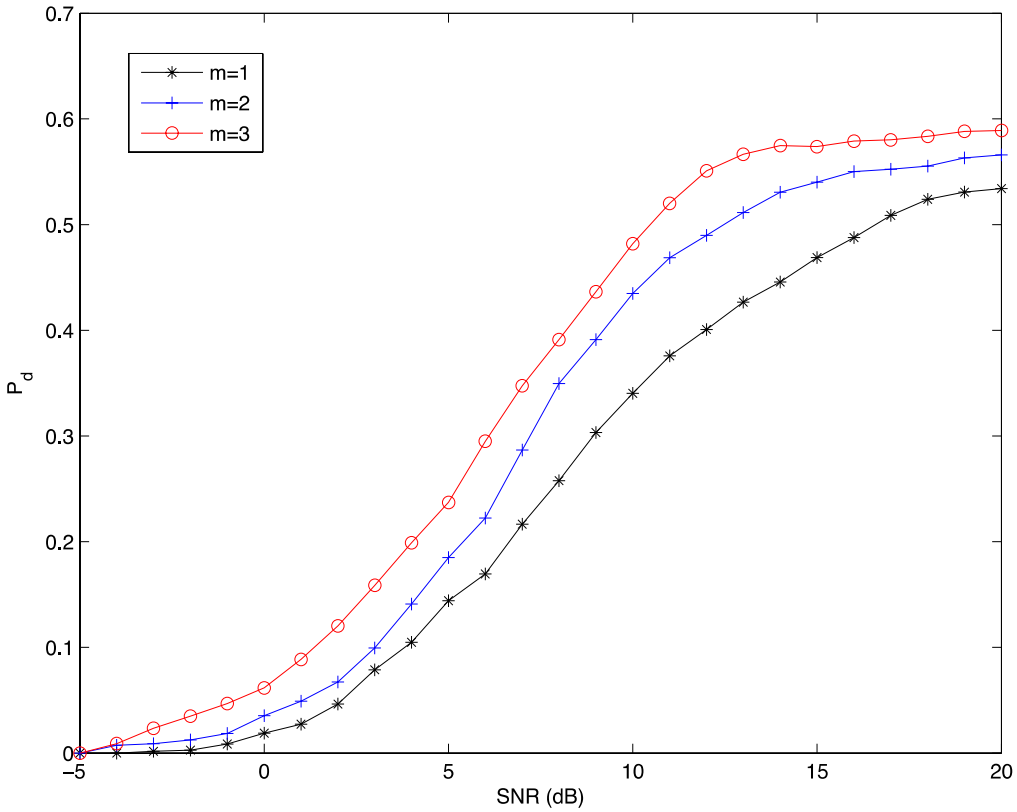

Fig. 9. P_d vs. SNR for varying m with L=2

Performance quantification

In Fig. 9, when SNR = 10 db, the P_d at m =2 shows a greater value than the P_d at m =1. Therefore, the gain in P_d by increasing the fading parameter from m =1 to m=2 is 28.09%. When SNR = 10 db, the P_d at m = 3 is higher than the P_d at m =2. The gain in P_d from m =2 to m =3 is 10.79%. Thus, an increase in the fading parameter m improves the performance of the sensor network.

3.4.4 Effect of number of sensors N

The P_d vs. N plots in Fig. 10 show the effect N(number of sensors) In Fig. 10 P_d is plotted versus N, the number of sensors deployed in a WSN. The fading parameter m is fixed at 3 and SNR = -5 to 20. With an increase in the antennas L at the sensors, the probability of detection P_d shows a drastic increase. The number of sensors N ranges from 0 to 15.

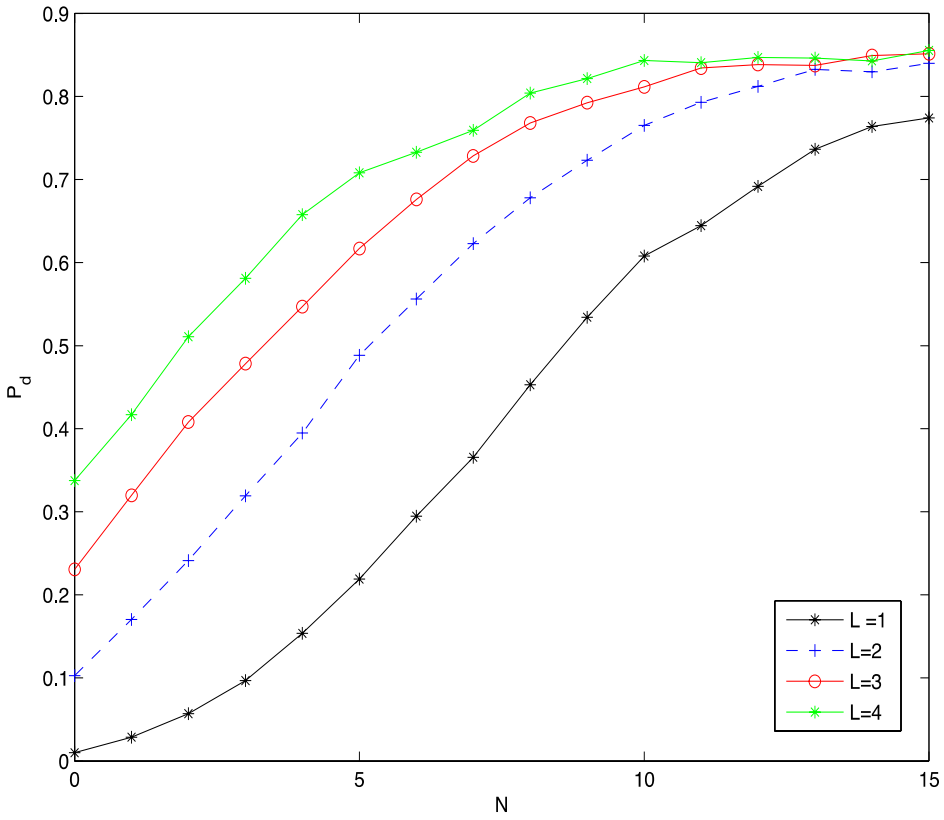

Fig. 10. P_d vs. N for varying L with m =3

Performance quantification

In Fig. 10, when N = 10 the value of P_d is greater than the value of P_d when N = 5 at L = 1. The gain in P_d by increasing N from 5 to 0 is 65.6%. This shows that in a WSN, numerous sensor nodes deployed in an environment that is to be sensed with multiple antennas at the sensors give good detection performanceP_d. The gain in P_d by increasing L from 1 to 2 is 61.2%.

3.4.5 Effect of probability of misdetection P_{md} against number of sensors N

In Fig. 11, a plot of the probability of misdetection P_{md} versus the number of sensor nodes N in a WSN is shown.

With P_{dk} = 0.5 and P_{fk} = 0.05 per sensor and a fixed number of antennas L = 2. The SNR ranges from -5 to 20.

$$P_{md} = 1 - P_d \tag{3.18}$$

As shown in (Fig. 11) , when the number of sensors increases, the P_{md} decreases gradually with an increase in the fading parameter m. So, the higher the value of m, the lower the misdetection in the WSN. A high value of P_{md} means the system performance is not a good in that particular WSN. Misdetection is caused by the false interpretation of data by the sensors because of the presence of interference from other signals and noise.

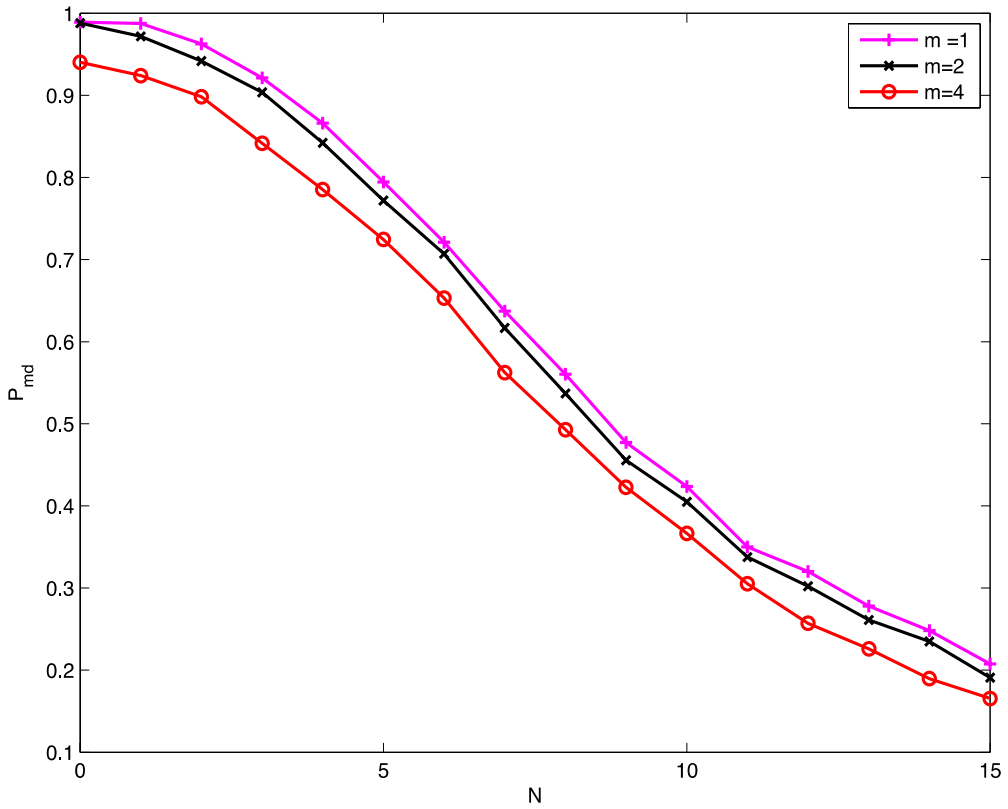

Fig. 11. P_{md} vs. N for varying m with L=2

Performance calculation from Fig. 11

When N = 5, P_{md} at L = 2 is 0.7945 [$m = 1$];When N = 5, P_{md} at L = 2 is 0.7719 [$m = 2$];When N = 5, P_{md} at L = 2 is 0.7244 [$m = 4$].

In (Fig. 11), the P_{md} decreases with an increasing value of m. The decrease in P_{md} with increasing m from 2 to 4 is 6.5%. So, the system must be designed with a high m value so that there is very little probability of misdetection.

3.5 Receiver operating Characteristics (ROC)

Receiver operating characteristics are represented by ROC curves in which the probability of detection (P_d) versus the probability of false alarm (P_f) illustrate the performance of the system, where P_d is the true positive rate (sensitivity) and P_f is the false positive rate (specificity). ROC curves show maximum performance at high SNR and moderate threshold. In the following ROC curves (Fig. 12–18), P_{dk} = 0.5 and P_{fk} = 0.05 per sensor. The threshold is set to a range of values -20 to +20 with steps of 0.5.

3.5.1 Effect of multiple antennas on ROC curves

Fig. 12 gives the ROC curves P_d versus P_f corresponding to fusion statistics LLR at channel SNR = 10 dB for Nakagami-*m* fading with a single sensor having multiple antennas L= 1, 2, 3. The total number of sensors is fixed at N = 8. The optimal LR-based fusion rule provides the uniformly most powerful detection performance, however it requires instantaneous CSI.

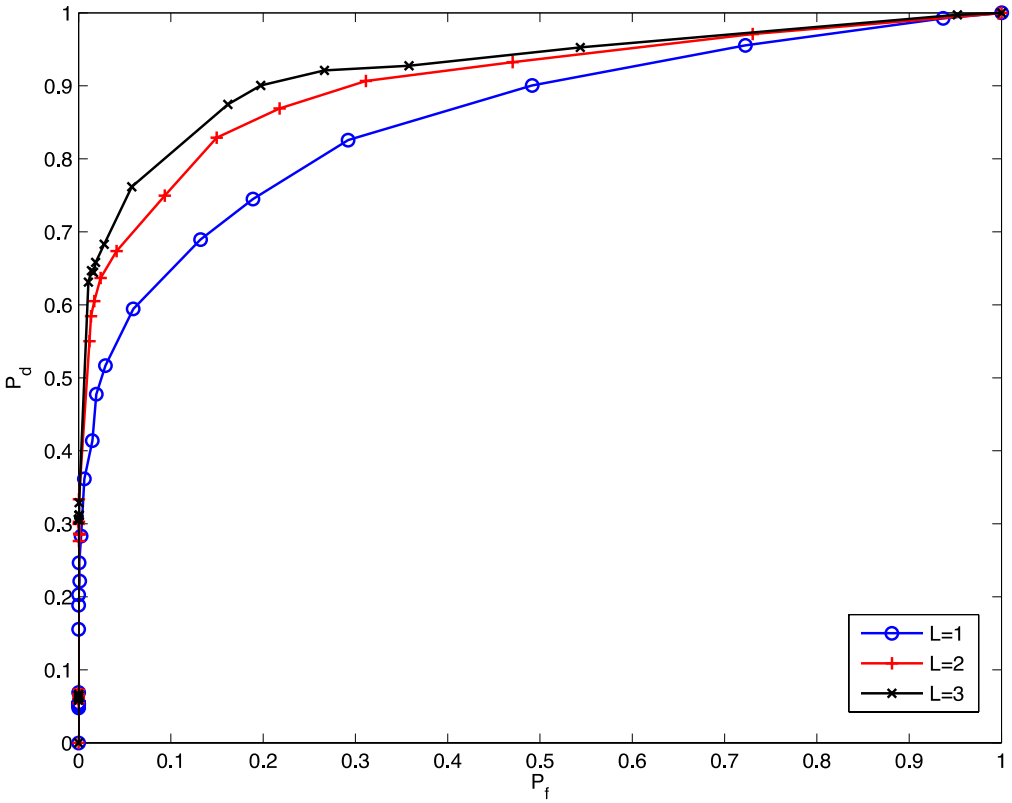

Fig .12. ROC curves for varying L with SNR=10 dB.

In Fig. 12 the value of P_f lies at 0 for most of the range of lower threshold values but gradually increases at moderate threshold values. Thus maximum detection probability occurs at lower threshold levels of P_d. Fig. 12 also shows a increase in P_d when the number of antennas L in the sensor node increases. In an ROC curve, the more the area under the curve (AUC), the better the WSN performance (more detection probability) of the system [25]. The AUC is the largest when L = 3. Thus, L = 3 provides a comparatively better P_d than L = 1 and L = 2.

3.5.2 Effect of fading parameter *m* on ROC curves

In Fig. 13, ROC curves—P_d versus P_f with varying values of m—corresponding to fusion statistics LLR at a channel SNR of 10 dB is shown. The number of antennas L = 2 is fixed and the total number of sensors is fixed at N = 4 with varying m values of {1, 3, 5}.

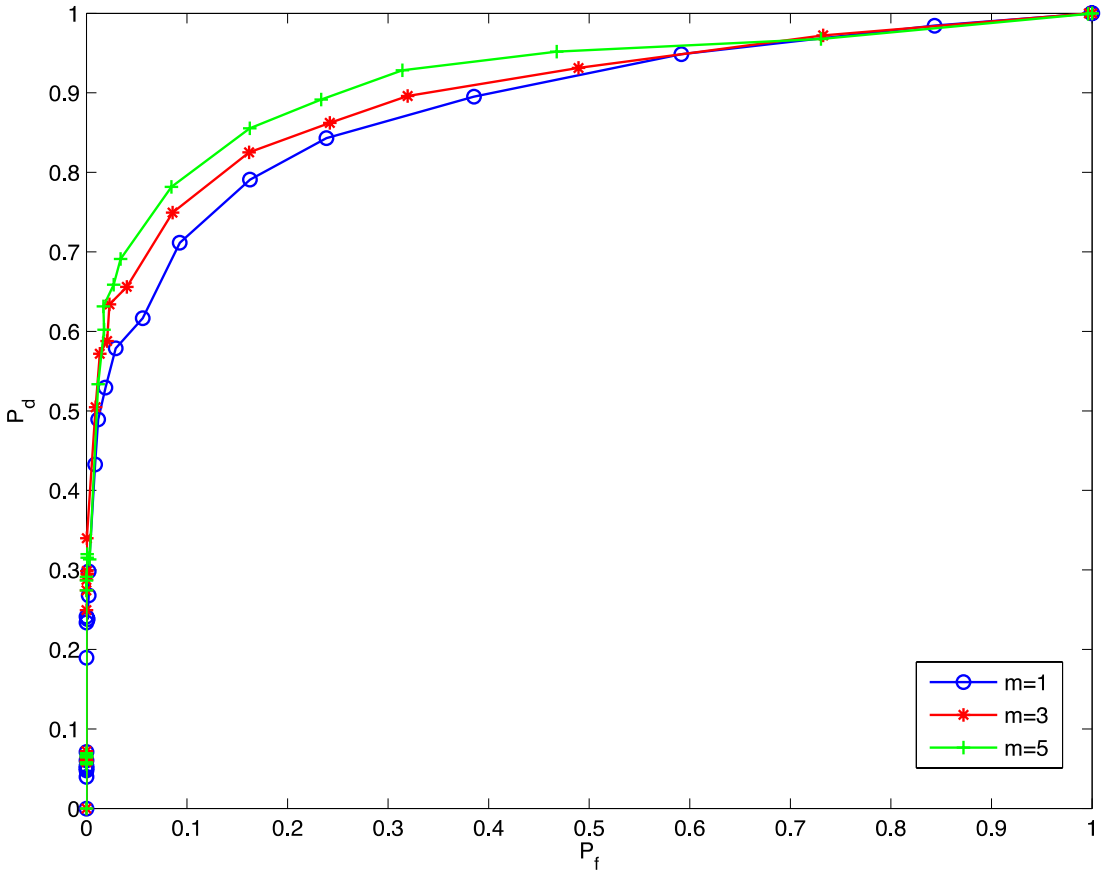

. Fig. 13. ROC curves for varying m with SNR=10 dB.

The simulated ROC graph in Fig. 13 shows a increase in P_d when the fading parameter *m* is increased. It has greater AUC when *m*=5 which gives the better P_d comparative to other m values *m*=3 and *m*=1.So higher the value of ***m*** better is the WSN performance.

3.6 Comparison of fusion schemes in the quest for high signal detection probability

This section involves in the comparison of various fusion schemes, both optimal and suboptimal fusion rules were deployed at the FC in the context of multiple antenna based sensor nodes. Although the optimum fusion rules provide better detection probability, these rules require much channel information which is costly to calculate. This motivates the creation of suboptimal fusion schemes. Our goal is to implement suboptimal fusion rules that do not require instantaneous CSI yet provide robust performance [1]. In [4], it is shown that for low-channel SNR, the maximal ratio combiner (MRC) is near-optimal. Interestingly, the very simple equal gain combiner (EGC) statistic, which requires a minimum amount of information, outperforms the MRC and is the most practical for moderate SNR values (i.e., $\sigma^2 = \infty$). The MRC is applicable for low SNR values and does not require knowledge of either P_{dk} or P_{fk}. The EGC provides better results than the MRC and outperforms the MRC in most SNR ranges. Simulation results are provided to confirm our analysis.

EGC: This is applicable when the moderate SNR values (i.e. $\sigma^2 = \infty$).

MRC: This is applicable for the low SNR values.MRC does not require knowledge of either P_{dk} or P_{fk}.EGC as comparative to MRC has provide better results and outperforms for most SNR range. Simulation results are provided to confirm our analysis

3.6.1 Comparison of LLR, MRC, EGC

3.6.1.1 P_d versus P_f comparison of LLR, MRC, EGC, with L = 2

The ROC plots of P_d versus P_f in Fig. 14 are generated corresponding to fusion statistics LLR, MRC, and EGC at a channel with an SNR of -5 dB. The number of antennas L is 2 on a single sensor. The total number of sensors N is 4. The fading parameter $m = 2$ per sensor.

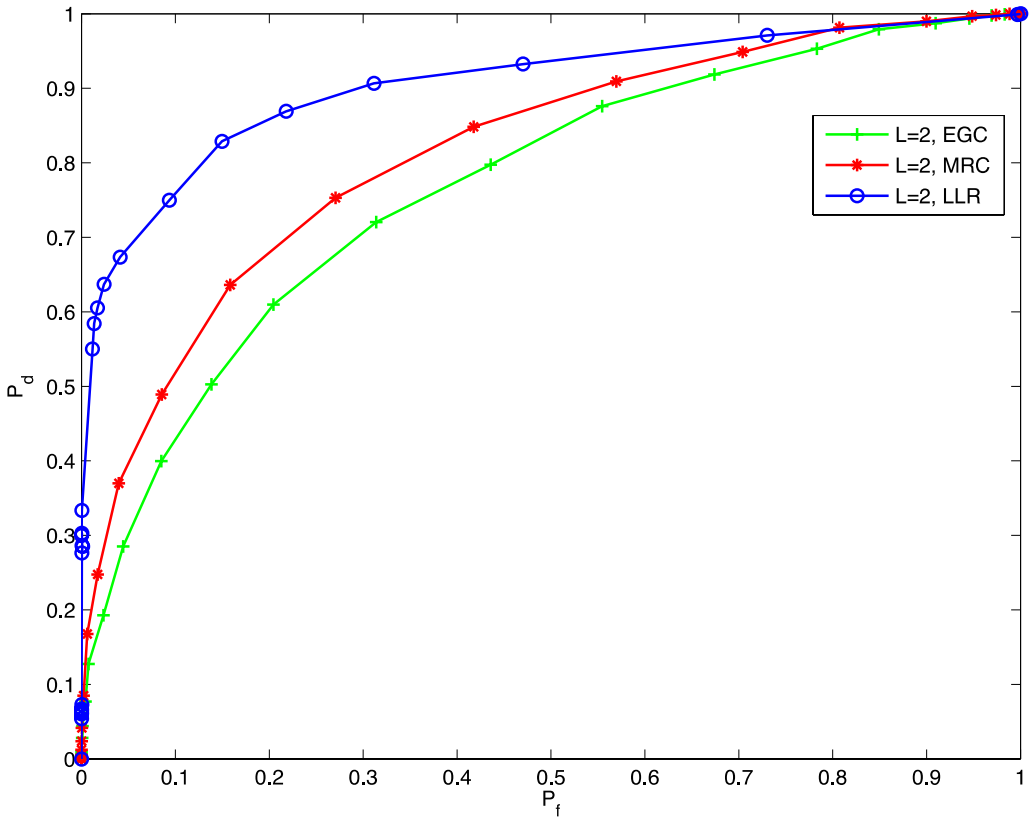

Fig. 14. ROC curves for LLR, EGC, MRC with L=2, with N=4, SNR=-5 dB, m=2.

In Fig. 14 the optimal and suboptimal rules are compared with respect to P_d versus P_f with L = 2. The simulated graph shows that the LLR outperforms both suboptimal rules EGC and MRC. We have simulated the ROC for the low SNR value of -5 dB, thus, the MRC outperforms the EGC.

3.6.1.2 Comparison of LLR, MRC, EGC, with L = 1 and L = 2

The Fig. 15 compares optimal and suboptimal fusion rules with single antenna and multiple antennas. With parameters SNR = -5 dB, N = 4, a threshold of -20 to +20 with steps of 0.5, L = 1, 2. L = 2 outperforms L = 1 in both optimal and suboptimal rules. Thus in any decision fusion rule, whether optimal or suboptimal, we achieve better detection probability by using multiple antennas at the sensor nodes.

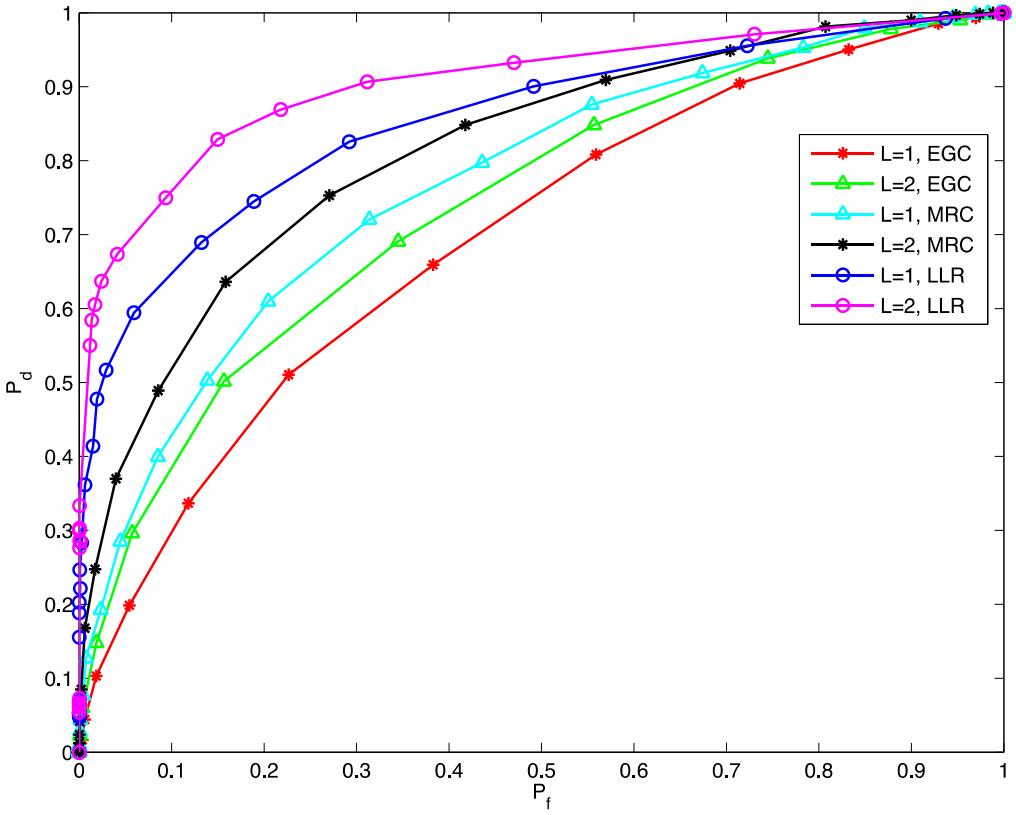

Fig. 15. ROC curves for fusion statistics LLR,EGC,MRC with comparison of L=1 and L=2 with N=4, SNR=-5 dB.

3.6.1.3 Comparison of MRC, EGC, for varying fading parameter *m*

In Fig. 16 with the same above criteria, ROC curves are generated with multiple antennas (i.e., L = 2) with varying values of m. Graphs are plotted with m = 1, m = 4 for the suboptimal fusion rules MRC, EGC.

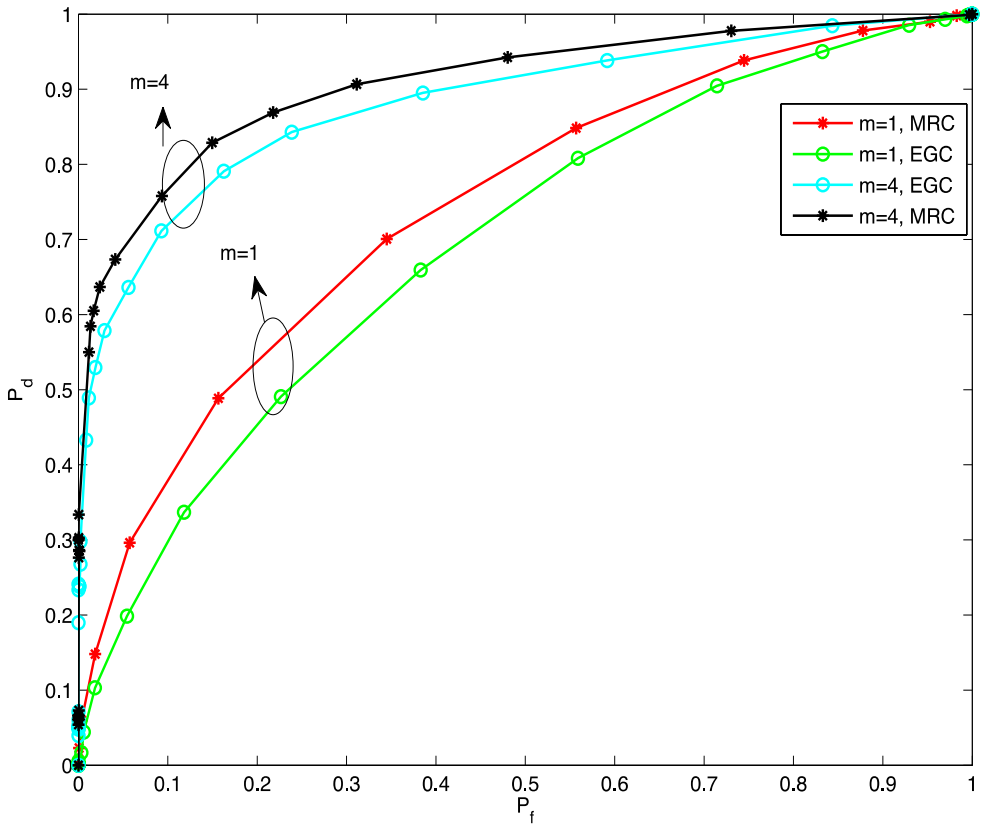

Fig. 16: ROC curves for various fusion statistics EGC, MRC with comparison of m=1 and m=4 with fixed N=4, SNR=-5 dB

The simulated ROC graph in Fig. 16 shows a increase in P_d when the fading parameter m is increased for the suboptimal fusion rules MRC and EGC. The AUC is larger when m = 4 which yields a better P_d compared to m = 1. However, in Fig. 16 the MRC outperforms the EGC as the values are plotted for a low SNR of -5 dB. Thus, the higher value of m yielded a better WSN performance.

3.6.2 Comparison of Optimal and Suboptimal fusion schemes with various SNR values

In Fig. 17, LLR, EGC, MRC are compared in the presence of SNR values of -10 dB, 0 dB, and 5 dB. L = 2, the threshold = -20 to 20 in steps of 0.5, N = 4, P_{dk} = 0.5, and P_{fk} = 0.05. The generation of MRC does not require this information. It is interesting to see how the curves behave with various SNR values.In Fig. 17 we observe that LLR outperforms EGC and MRC for all three SNR values: -10, 0, and 5 dB. As shown in Fig. 16, MRC has better detection probability P_d at very low SNR values. When SNR is 0 dB, MRC and EGC slightly overlap initially at high threshold values (lower values of P_d and P_f) and gradually EGC outperforms MRC as EGC performs better at moderate SNRs.

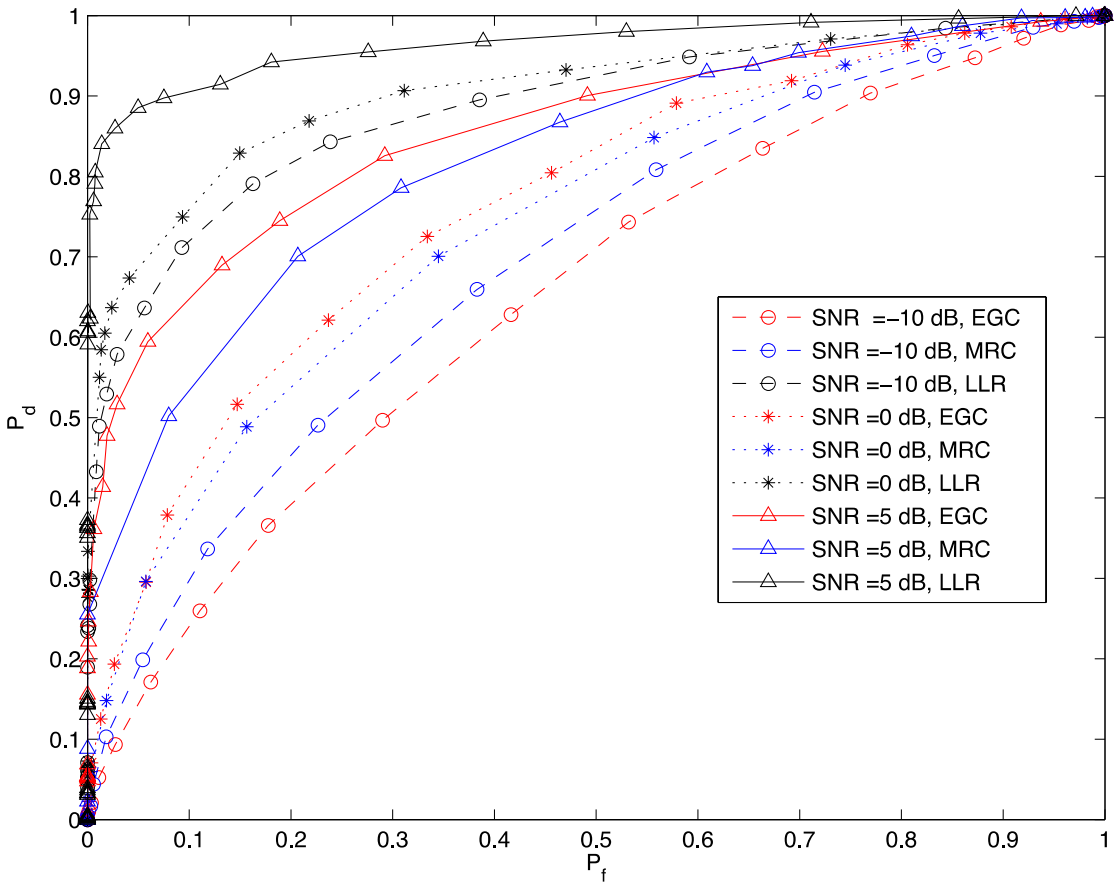

Fig. 17: ROC curves for various fusion statistics LLR, EGC, MRC for SNR {-10,0,5} (dB) with L=2 with N=4.

When the SNR is 5 dB (a moderate value in this scenario) the EGC performs better than the MRC. Fig. 17 shows that the LLR provides the best P_d (detection probability) at all SNR values. Fig. 17 also conveys that the higher the SNR, the better the WSN system performance. Fig. 15 and Fig. 17 both show that with both optimal and suboptimal decision fusion schemes at the FC, the LLR provides the best WSN performance, however, the LLR requires a lot of channel information.

3.7 Conclusion

In this chapter the effect of multiple antennas on WSN's and comparison of optimal and suboptimal decision fusion rules is characterized. The effect of implementing multiple antennas at the WSN's is studied through various numerical and simulation results. Our results show that, using multiple antennas and with higher values of the fading parameter m makes a better improvement in the detection performance by mitigating the impact of fading channels. Next case involves in comparing the optimal and suboptimal decision fusion rules. The results shows that in all cases the optimal fusion rule has better performance gains than the suboptimal fusion rules. In case of suboptimal fusion rules the MRC, EGC shows a better performance gain in high SNR values and low SNR values respectively.

Chapter 4

Conclusion and Future Work

The project aims to improve the overall reliability of detection of a WSN operating in a wireless multipath fading environment by deploying multiple antennas at the sensor nodes. Multiple antenna based sensors may be deployed, for example, in the IEEE 802.11 networks [5], which are widely used for residential, business and industrial applications for general LAN access in work areas and use multiple input, multiple output antennas. Thus, characterization of the detection performance of the WSN with multiple antenna based sensing nodes in generic fading would ultimately aid in the design and analysis of practical sensor systems which would further help in the innovation of efficient detection systems that are more robust to the fading environments. Motivated by this fact, distributed detection and fusion of data transmitted over wireless fading channel with different fading severity is considered by modeling the wireless channel as Nakagami-*m* faded. To mitigate the impact of fading, implementation of multiple antennas at the sensor nodes to quantify the possible improvement in the signal detection performance is considered. The optimal LLR-based fusion rule is derived with the resulting numerical results indicating a remarkable improvement in the detection performance of the multiple antenna based WSN compared to single antenna based WSN. Since the optimal LLR requires a knowledge of the channel statistics, sub-optimal MRC and EGC rules are considered as well. Simulation results show that the EGC rule is better compared to the MRC rule in moderate to high SNR regime while the MRC outperforms the EGC in low SNR regions. Nevertheless, both the sub-optimal rules still yield prominent performance gains in multiple antenna based WSN compared to the single antenna based WSN.

As further extension of the current work, the effect of other non-cooperating sensor nodes which may cause interference at the fusion center thus making the current fusion rules impractical or erroneous, could be considered. This would demand the need of design and analysis of new fusion rules that can mitigate the impact of interference in decision making. Another extension could be the consideration of a strong dominant line-of-sight reception at the fusion center directly from the signal to be detected. Such scenario may arise when a dedicated radio-frequency repeater station is deployed between the transmit signal source and the fusion center. The consideration of Rician fading model may be interesting to model the wireless propagation in such situations.

References

[1] R.Niu, B.Chen and P.Varshney, "Fusion of decisions transmitted over Rayleigh fading channels in wireless sensor networks," *IEEE Trans. Signal Process*., vol.54, no.3, pp.1018-1027, Mar. 2006.

[2] V. A. Aalo and G. P. Efthymoglou, "Decision Fusion schemes for wireless sensor networks operating in a Nakagami-m fading environment," in *Proc. IEEE Int. Symp. on Personal, Indoor and Mobile Radio Communications (PIMRC),* 2009.

[3] M. K. Simon and M.-S. Alouini, "Digital communications over fading channels (M.K. Simon and M.S. Alouini; 2005) [book review]," *IEEE Trans. Inf. Theory*, vol. 54, no. 7, pp. 3369–3370, Jul. 2008.

[4] B. Chen, R. Jiang, T. Kasetkasem and P.K. Varshney, "Fusion of decisions transmitted over fading channels in wireless sensor networks," in *Proc. Asilomar Conf. on Signals, Systems and Computers,* April 2002.

[5] S. C. Mukhopadhyay and H. Leung, *Advances in Wireless Sensors and Sensor Networks,* Springer Verlag Berlin Heidelberg, May 2010.

[6] Eugene Y.Song and Kang B.Lee, *IEEE* 1451.5 Standard-Based Wireless Sensor Networks, National Institute of Standards and Technology, Gaithersburg, Maryland USA

[7] Rabaey, M Ameer, J. Silva, L.D.Patel, S.Roundy," Picoradio, and supports ultra low hoc wireless power, Computer networking," July 2000.

[8] Guibas, Leonidas and Zhao, Feng, Wireless Sensor Networks: An Information Processing Approach, Morgan Kaufman Publishers, San Francisco, CA, Oct. 2004 .

[9] C. Chong and S. Kumar, "Sensor networks: evolution, opportunities, and challenges," *Proc. IEEE*, pp.1-10, Aug. 2003

[10] Feng Wang; Jiangchuan Liu, "Networked Wireless Sensor Data Collection: Issues, Challenges, and Approaches," *IEEE Trans. Wireless Commun.*, pp.1-14, 2011.

[11] Namrata Atre and Dhiiraj Nitnawrre, " *Comparitive analysis of channel fading models in wireless," sensor networks*, *IEEE Trans. Signal Process*., vol.3, Issue.4, Apr. 2013.

[12] M. C. Necker and G. L. Stuber, **"** Totally blind channel estimation for OFDM on fast varying mobile radio channels,**"** *IEEE Trans. Wireless Commun.*, pp. 1– 11, Sep. 2004.

[13] Hao Xie-Dong; Liu Ai-Jun; Zhang Bang-Ning, "Performance improvement using beam diversity technique in GEO satellite communication system over correlated Nakagami-m fading channels," *Microwave and Millimeter Wave Technology., Int. Conf. on* , pp. 1-6 April 2008.

[14] Halperin, Daniel, Wenjun Hu, Anmol Sheth, and David Wetherall, " 802.11 with multiple antennas for dummies." *ACM SIGCOMM Computer Commun.* pp. 1-6,2010.

[15] Liu, Chi Harold, Kin K. Leung, and Athanasios Gkelias. "A novel cross-layer QoS routing algorithm for wireless mesh networks." *IEEE Int. Conf. Commun. (ICC) on*, pp. 1-5, 2008.

[16] Li, X. Rong, Yunmin Zhu, Jie Wang, and Chongzhao Han. "Optimal linear estimation fusion. I. Unified fusion rules." *IEEE Trans. Info. Theory*, pp 1-18, 2003.

[17] Z. Chair and P. K. Varshney, "Optimal data fusion in multiple sensor detection systems," *IEEE Trans. Aerosp. Electron. Syst.*, vol. AES-22, no.1, pp. 1-3, Jan. 1986.

[18] S. K. Jayaweera, "Large system decentralized detection performance under communication constraints," *IEEE Commun. Lett.*,pp. 1-5, Sep. 2005.

[19] I. S. Gradshteyn and I. M. Ryzhik, *Table of Integrals, Series, and Products*, 7th ed. New York: Academic, 2007.

[20] Available [online] at: http://en.wikipedia.org/wiki/Nakagami_distribution

[21] Available [online] at: http://www.awe-communications.com/Propagation/MIMO/

[22] Mietzner, J.; Schober, R.; Lampe, L.; Gerstacker, W.H.; Hoeher, P.A., "Multiple-antenna techniques for wireless communications - a comprehensive literature survey," *IEEE Trans. Wireless. Commun.*, pp.1-18, 2009.

[23] Available [online] at: http://www.cs.fsu.edu/~mascagni/Advanced_Monte_Carlo_Methods.html

[24] Ali, Q.I.; Abdulmaowjod, A.; Mohammed, H.M., "Simulation & performance study of wireless sensor network (WSN) using MATLAB," *Energy, Power and Control (EPC-IQ), Int. Conf. on*, pp.1-7, Dec. 2010.